

Interacting electrons on a quantum ring: accuracy and optimization of the Jastrow-Slater wave function for local and nonlocal Hamiltonians

S. S. Gylfadottir, A. Harju, T. Jouttenus, and C. Webb

Laboratory of Physics, Helsinki University of Technology, P. O. Box 4100 FIN-02015 HUT, Finland

(Dated: October 21, 2019)

We study a system of interacting electrons on a one-dimensional quantum ring using the exact diagonalization and the variational quantum Monte Carlo method. We examine the accuracy of the Slater-Jastrow -type many-body wave function for the Coulomb-type interaction between electrons. We compare energies, occupation numbers, and pair correlation functions obtained from the two approaches. Our results show that this wave function captures most correlation effects. The performance for the closed-shell cases is slightly better than for the open-shell ones. For the non-local contact interaction between electrons, we show how to evaluate the expectation value of the interaction in a Monte Carlo scheme, and derive a formula for the wave function optimization.

PACS numbers: 71.10.Pm, 73.22.-f, 02.70.Ss

I. INTRODUCTION

Various low-dimensional electron systems have been the subject of considerable scientific interest for more than two decades. Examples of these structures can be formed in a two-dimensional electron gas by applying appropriate confinement, thus restricting the motion of electrons to a small area on the boundary between two semiconducting materials. These systems are in many ways similar to atoms, however, their properties can be controlled by adjusting their geometry, the external confinement, and applied magnetic field. Nanostructures are a source of discoveries of novel quantum phenomena which do not appear in atoms. They are important both in connection with potential device applications and can function as convenient samples to probe the properties of many-electron systems in reduced dimensions.

In quantum rings, electrons are confined to move on a circular region in space. They have many interesting and actively explored properties: Under the influence of a magnetic field, an equilibrium current flows along the ring. Furthermore, the energy spectrum is periodic in the magnetic flux with a period of the flux quantum $\Phi_0 = h/e$ in case of an even number of noninteracting electrons, but $\Phi_0/2$ for an odd number. Recently, the existence of an interaction-driven fractional periodicity has been discovered both in experiments^{1,2} as well as in theoretical and computational studies.^{3,4,5,6,7,8,9} This is often referred to as the fractional Aharonov-Bohm effect.

In this paper we study the accuracy of a variational quantum Monte Carlo (VMC) approach, using the Jastrow-Slater wave function, to quantum ring systems. This approach has been found to be extremely accurate in the case of quantum dots.¹⁰ The main advantages of quantum Monte Carlo (QMC) methods are their applicability to large electron systems and their accuracy in capturing electron-electron correlation effects. To date, very few QMC studies of the electronic properties of nanoscale semiconductor quantum rings have been done. Emperador *et al.* investigated the fractional Aharonov-Bohm effect in few-electron quantum rings using multi-

configurational diffusion Monte Carlo⁸ and Borrman and Harting used path integral Monte Carlo to study the transition between spin ordered and disordered Wigner crystal rings.¹¹

We calculate using VMC the ground state energy, occupation distribution and pair distribution function of the quantum ring, in zero magnetic field, containing from two to six interacting electrons. The interaction is taken to be Coulombic. To test the accuracy of our approach we perform exact diagonalization (ED) calculations and compare the results. In most cases considered here, VMC gives a very accurate estimate of the ground state energy, the only exception being when the configuration of the system is an open-shell, where it still gives reasonably good results. VMC captures the occupation distribution very accurately, as well as the pair distribution function. The only case where there are considerable differences in the latter is for an anti-ferromagnetic configuration of six electrons. Here VMC does not capture the long-range part of the electron-electron correlation very well. We also show how the nonlocal contact interaction can be treated within a VMC scheme, especially how the wave function optimization^{12,13,14} can be done for a nonlocal Hamiltonian. Finally we consider a simple mapping between the Coulomb and contact interactions which can be applied to quantum rings with fair accuracy at low interaction strength.

This paper is divided as follows. In section II we discuss our model of the quantum ring system and go in considerable detail through the two methods used to calculate its ground state properties, ED and VMC. Then the results for the Coulomb interaction are presented in Section IIIA, those for the contact interaction in Section IIIB and finally we describe the mapping between the two types of interaction in Section IIIC. A summary and our conclusions follow in Section IV.

II. MODEL AND METHODS

A. Model

We model the semiconductor quantum rings in the effective mass approximation by a many-body Hamiltonian

$$\mathcal{H} = -\frac{\hbar^2}{2m} \sum_{i=1}^N \frac{\partial^2}{\partial \theta_i^2} + \sum_{i < j}^N V(\theta_{ij}) , \quad (1)$$

where θ_i is the angular coordinate of the i th electron and $V(\theta_{ij})$ is the interaction potential between two electrons. We assume that the ring is extremely narrow so that the electrons can only move at a certain radius, leading to a purely one-dimensional ring. We will treat two types of interaction, a Coulombic and a contact interaction. The Coulomb interaction for a ring system is written as

$$V(\theta_{ij}) = \frac{V_C}{R\sqrt{4\sin^2(\theta_{ij}/2) + \mu^2}} , \quad (2)$$

where R is the radius of the ring, V_C controls the strength of the interaction, and μ is a small parameter that eliminates the singularity at $\theta_{ij} = 0$. In a sense, it gives the ring a finite width of μR , making it possible for electrons to pass each other. The contact interaction with strength V_δ is defined as

$$V(\theta_{ij}) = 2\pi V_\delta \delta(\theta_{ij}) . \quad (3)$$

The single-particle eigenstates of the noninteracting case are plane waves

$$\psi_l(\theta) = \exp(-il\theta)/\sqrt{2\pi R} ,$$

with energies

$$\varepsilon_l = \frac{\hbar^2}{2mR^2} l^2 ,$$

where $l = 0, \pm 1, \pm 2, \dots$ is the angular momentum quantum number. We scale the units so that the energy is measured in units of $E_0 = \hbar^2/(2m\pi^2R^2)$ and length in units of R . The only parameter which is tuned is the interaction strength, and for the Coulomb interaction this can be translated into a change of the ring radius by the following formula

$$V_C = \frac{R}{2a_B^*} , \quad (4)$$

where a_B^* is the effective Bohr radius. The results presented in this paper are for interaction strength in the range of 0.1 to 10, which corresponds to a radius of 2.1 nm to 209 nm assuming GaAs material parameters. For comparison, the quantum ring system studied by Keyser *et al.*^{1,15} had a radius of around 150 nm, which corresponds to an interaction strength of $V_C = 7.2$ in our units. The width of their ring can be estimated to be around 20 nm, which is in reasonable agreement with the value of $\mu = 0.1$ used in this work.

B. Exact diagonalization

The exact diagonalization method (ED), originally called configuration interaction, is a systematic scheme to expand the many-particle wave function using the non-interacting states as a basis. This method traces back to the early days of quantum mechanics, to the work of Hylleraas.¹⁶ The calculation of matrix elements for the many-body case was originally derived by Slater and Condon,^{17,18,19} and developed further by Löwdin.²⁰ The use of the term ED for this can then be seen as an attempt to replace the term configuration interaction with a normal mathematical term.²¹ This term might in some cases be misleading, as truly exact results are obtained only in the limit of an infinite basis.

As a simple example to start from, consider a single-particle Hamiltonian split into two parts $\mathcal{H} = \mathcal{H}_0 + \mathcal{H}_I$, where the Schrödinger equation of the first part is solvable:

$$\mathcal{H}_0 \phi_i(\mathbf{r}) = \varepsilon_i \phi_i(\mathbf{r}) , \quad (5)$$

and the wave functions $\phi_i(\mathbf{r})$ form a orthonormal basis. The solution of the full Schrödinger equation can be expanded in this basis as $\psi(\mathbf{r}) = \sum_i \alpha_i \phi_i(\mathbf{r})$. Inserting this into the Schrödinger equation

$$\mathcal{H}\psi(\mathbf{r}) = E\psi(\mathbf{r}) , \quad (6)$$

results in

$$(\mathcal{H}_0 + \mathcal{H}_I) \sum_i \alpha_i \phi_i(\mathbf{r}) = E \sum_i \alpha_i \phi_i(\mathbf{r}) . \quad (7)$$

Using Eq. (5), multiplying with ϕ_j^* and integrating gives

$$\sum_i \alpha_i \varepsilon_i \delta_{ij} + \sum_i \alpha_i \int \phi_j^*(\mathbf{r}) \mathcal{H}_I \phi_i(\mathbf{r}) d\mathbf{r} = E \sum_i \alpha_i \delta_{ij} \quad (8)$$

for every j . This can be written as a matrix equation

$$(\mathcal{H}_0 + \mathcal{H}_I) \boldsymbol{\alpha} = E \boldsymbol{\alpha} , \quad (9)$$

where \mathcal{H}_0 is a diagonal matrix whose i th element is ε_i , and the j th element of \mathcal{H}_I is $\int \phi_j^*(\mathbf{r}) \mathcal{H}_I \phi_i(\mathbf{r}) d\mathbf{r}$. The vector $\boldsymbol{\alpha}$ contains the values α_i . In this way, the Schrödinger equation can be mapped to a matrix form. In principle, the basis $\{\phi_i\}$ is infinite, but the calculations are done in a finite basis. The main computational task is to calculate the matrix elements of \mathcal{H}_I and to diagonalize the matrices. The convergence of the expansion depends on the actual values of the matrix elements, and in the case where \mathcal{H}_I is only a small perturbation to \mathcal{H}_0 it is fastest.

In a similar fashion, one can split the many-particle Hamiltonian into two parts, typically a noninteracting and an interacting one. The solution to the noninteracting many-Fermion problem is a Slater determinant formed from the N lowest energy eigenstates of the single-particle Hamiltonian. The basis typically chosen

for the interacting problem is a Slater determinant basis constructed from M single-particle states. For an N -particle problem, $\binom{M}{N}$ different many-particle configurations can be constructed by occupying any N of the M available states. Each of these determinants is labeled by the N indices of the occupied single-particle states. Due to interactions, other configurations than the one of the noninteracting ground state have a finite weight in the expansion of the many-particle wave function.

The Schrödinger equation maps to matrix form in a similar way as in the preliminary example above. The calculation of the matrix elements of the Hamiltonian are simpler using second quantization and the occupation number representation. We will only state the results here.

The noninteracting Hamiltonian matrix H_0 in the determinant basis is diagonal with the i th element equal to $E_i = \sum_{j=1}^N \varepsilon_{ij}$, where ij labels the occupied single-particle state. The elements of the interaction Hamiltonian matrix can be found by a straight-forward calculation using the anti-commutation rules of the creation and annihilation operators. The only non-zero matrix elements are between configurations that differ at most by two single-particle occupations. If both of the two configurations have two single-particle states occupied that are unoccupied in the other one, the interaction matrix element is

$$\pm(V_{pqrs} - V_{pqsr}) , \quad (10)$$

where p and q are single-particle states occupied in the left configuration and unoccupied in the right one, and similarly for s and r with right and left interchanged. The sign of the matrix element depends on the total number of occupations between p and r and between q and s due to anti-commutation of the creation and annihilation operators. If this number is odd, the sign is minus, otherwise plus. For the Coulomb interaction

$$\begin{aligned} V_{ijkl} &= \int \phi_i^*(\mathbf{r}_1) \phi_j^*(\mathbf{r}_2) \frac{1}{r_{12}} \phi_k(\mathbf{r}_1) \phi_l(\mathbf{r}_2) d\mathbf{r}_1 d\mathbf{r}_2 \\ &\times \delta_{s_i, s_k} \delta_{s_j, s_l} , \end{aligned} \quad (11)$$

and the delta functions result from the spin part summation. In the case of a one-dimensional quantum ring this matrix element has a closed form

$$V_{ijkl} = \frac{1}{\pi} Q_{i-k-\frac{1}{2}}(\mu^2/2 + 1) , \quad (12)$$

where $Q(x)$ is the Legendre function which can be written in terms of Gauss's hypergeometric function.

If the two configurations have a difference of only one occupation, the final result for the interaction matrix elements is

$$\pm \sum_i (V_{qiri} - V_{qir}) , \quad (13)$$

where q is occupied in the left configuration and unoccupied in the right one, and for r the other way around.

The sum over i is over orbitals that are occupied in both configurations. Again the sign of the matrix element depends on number of occupations between the differing orbitals. The Coulomb matrix element V_{qiri} is zero when the system in question is rotationally symmetric, as is the case for a quantum ring.

The diagonal elements of the interaction Hamiltonian matrix are

$$\sum_{i < j}^N (V_{ijij} - V_{ijji}) . \quad (14)$$

To summarize, the noninteracting part results in a Hamiltonian matrix which is diagonal, and the interaction Hamiltonian couples configurations that differ by at most two occupations. Now that we know the Hamiltonian matrix elements, we can sketch the basic ED procedure as follows: First solve for M eigen-pairs of the single-particle Hamiltonian \mathcal{H}_0 . After those have been found, calculate the two-particle matrix elements V_{ijkl} of Eq. (11). Construct the $\binom{M}{N}$ N -particle configurations from M single-particle states. Here configurations with wrong symmetry can be rejected. For example, one can pick only configurations with certain z -component of the total spin or some other good quantum number, like the angular momentum in our case. To construct the Hamiltonian matrix, calculate the interaction matrix elements of the Hamiltonian \mathcal{H}_I between the configurations. Construct the diagonal noninteracting Hamiltonian matrix elements from the single-particle eigenvalues. Finally, diagonalize the Hamiltonian matrix. The main problem of the ED method is the exponential computational scaling of the method as a function of the number of particles. An other problem is the convergence rate as a function of basis size.

To compare the ED and VMC methods for the ring, we look at the pair distribution function and the angular momentum distribution of the electrons in the ring, in addition to the ground state energy. The pair distribution function of the system is defined by

$$\begin{aligned} n_\sigma(\mathbf{r}) n_{\sigma'}(\mathbf{r}') g_{\sigma\sigma'}(\mathbf{r}, \mathbf{r}') \\ = \langle \psi | \Psi_\sigma^\dagger(\mathbf{r}) \Psi_{\sigma'}^\dagger(\mathbf{r}') \Psi_{\sigma'}(\mathbf{r}') \Psi_\sigma(\mathbf{r}) | \psi \rangle , \end{aligned} \quad (15)$$

where $n_\sigma(\mathbf{r})$ is the spin σ particle density and $\Psi_\sigma^\dagger(\mathbf{r})$ and $\Psi_\sigma(\mathbf{r})$ are the field operators. It describes the probability that, given an electron of spin σ at \mathbf{r} , an electron of spin σ' is found at \mathbf{r}' . It therefore gives an idea of the strength of correlation between electrons. The pair distribution function can be derived in a similar way as the Coulomb matrix elements using the anti-commutation rules of the creation and annihilation operators. The occupation distribution can be calculated easily using

$$f(l, \sigma) = \sum_i n_{l\sigma}^{(i)} |\alpha_i|^2 , \quad (16)$$

where the sum over i runs over all Slater determinants in the many-body basis and $n_{l\sigma}^{(i)}$ is 1 if the single-particle

state $\phi_l(\theta)$ in the i th Slater determinant is occupied by an electron of spin type σ , otherwise it is zero. The distribution $f(l, \sigma)$ gives the probability that an electron of spin σ has angular momentum l .

C. Variational Monte Carlo method

The QMC methods are among the most accurate ones for tackling a problem of interacting quantum particles.²² Often the simplest QMC method, namely, the variational QMC (VMC), is able to reveal the most important correlation effects. In many quantum systems, further accuracy in, e.g., the energy is needed, and in these cases methods such as the diffusion QMC allow one to obtain more accurate estimates for various observables.

The VMC strategy of solving the ground state of an interacting system of N particles (defined by the Hamiltonian operator \mathcal{H} and the particle statistics) starts by constructing the variational many-body wave function Ψ . Then, all the observables of the system can be computed from it. For example, the energy E , which is higher than the ground state energy E_0 , can be obtained from the high-dimensional integrals

$$E_0 \leq E = \frac{\int \Psi^*(\mathbf{R}) \mathcal{H} \Psi(\mathbf{R}) d\mathbf{R}}{\int |\Psi(\mathbf{R})|^2 d\mathbf{R}} ,$$

where \mathbf{R} is a vector containing all the coordinates of the N particles. If the particles have d degrees of freedom, the integrals here are $N \times d$ dimensional. As one would like to have N reasonable large, the integrals are typically so high-dimensional that these are most efficiently calculated using a Monte Carlo strategy. This is based on the limit

$$\lim_{N_R \rightarrow \infty} \frac{1}{N_R} \sum_{i=1}^{N_R} f(\mathbf{R}_i) = \frac{1}{V} \int_V f(\mathbf{R}) d\mathbf{R} ,$$

where the points \mathbf{R}_i are uniformly distributed throughout the volume V . The error in the evaluation of the integral decays as $\propto \sigma_f / \sqrt{N_R}$, where σ_f is the standard deviation of the function f . A typical trick to reduce the error is to make σ_f smaller by dividing the function f by a similar function g (that we assume to integrate to one). Then, one can rewrite the sum as

$$\begin{aligned} \frac{1}{N_R} \sum_{i=1}^{N_R} f(\mathbf{R}_i) &= \frac{1}{N_R} \sum_{i=1}^{N_R} g(\mathbf{R}_i) \frac{f(\mathbf{R}_i)}{g(\mathbf{R}_i)} \\ &= \frac{1}{N_R} \sum_{i=1}^{N_R} \frac{f(\mathbf{R}_i^g)}{g(\mathbf{R}_i^g)} , \end{aligned} \quad (17)$$

where now the points \mathbf{R}_i^g are distributed as g . The error in this approach is now smaller, as the function g was chosen such that the standard deviation of f/g is smaller than that of f .

Now in VMC, one typically generates the random set of N_R coordinates $\{\mathbf{R}_i\}_{i=1}^{N_R}$ so that they are distributed according to $|\Psi|^2$, and one obtains for the energy

$$E = \frac{1}{N_R} \sum_{i=1}^{N_R} \frac{\mathcal{H} \Psi(\mathbf{R}_i)}{\Psi(\mathbf{R}_i)} = \frac{1}{N_R} \sum_{i=1}^{N_R} E_L ,$$

where we have defined the local energy E_L to be

$$E_L = \frac{\mathcal{H} \Psi(\mathbf{R}_i)}{\Psi(\mathbf{R}_i)} .$$

One should note that E_L is a function of the coordinates, and it defines the energy at this point in space. If the wave function Ψ solves the Schrödinger equation, E_L equals the true energy of the system. From the Monte Carlo point of view, the error in determining the energy is related to the standard deviation of the local energy, and for this reason the statistical error in the VMC energy decreases as the wave function becomes more accurate.

The sampling of the random points \mathbf{R}_i can be done by, e.g., using the basic Metropolis algorithm. In that, the ratio of the sampling function at the i th and the previous step: $|\Psi(\mathbf{R}_i)|^2 / |\Psi(\mathbf{R}_{i-1})|^2$, needs to be calculated and the trial step is accepted if the ratio is larger than a uniformly distributed random number between zero and one.

A typical, and also the most commonly used VMC trial many-body wave function, is the one of a Slater-Jastrow type:

$$\Psi = D_\uparrow D_\downarrow e^J , \quad (18)$$

where the two first factors are Slater determinants for the two spin types, and

$$J = \sum_{i < j} j(\theta_{ij}) , \quad (19)$$

where $j(\theta_{ij})$ is a Jastrow two-body correlation factor. The determinants contain N single-particle orbitals, where the ones in different spin determinants can be the same. These determinants solve in some cases a noninteracting or a mean-field Schrödinger equation, but in general, one can choose these orbitals rather freely. This form of a wave function has proved to be very accurate in many cases.²² In quantum dots, the Jastrow-Slater wave function captures most correlation effects very accurately.¹⁰ The only possible exceptions are found in the fractional quantum Hall effect regime, where only some of the states can be well approximated by the Jastrow correlation. Interesting examples of successful cases are the Laughlin states.²³

We neglect the three-body and higher correlations in J , but one can easily generalize the Jastrow part to also contain higher-order correlations. This might not be very important in the present case, as we are studying a one-dimensional system. By lowering the dimensionality of the problem, correlation effects are enhanced, because

particles have less degrees of freedom to avoid each other. On the other hand, the lowered dimensionality makes it more difficult for more than two particles to get close to each other, and in this way the relative importance of correlations beyond the two-particle level decreases as the dimensionality is lowered.

One can also generalize the Jastrow-Slater wave function to contain more than one determinant per spin type. This leads to an increased computational complexity, and for this reason it is often avoided. Another generalization can be to replace the single-particle coordinates in the determinants by a set of collective coordinates, e.g., $\mathbf{r}_i \rightarrow \mathbf{r}_i - F(\{\mathbf{r}_j\}_{j=1}^N)$. This also leads to complications, this time in the calculation of the ratio of the wave functions in the Metropolis algorithm.

The determinants in our VMC trial wave function are constructed from the noninteracting single-particle states, and for the two-body Jastrow factor we use here a simple form of

$$j(\theta) = \frac{a - a \cos(\theta)}{2 + b + b \cos(\theta)}, \quad (20)$$

where a and b are variational parameters, different for electron pairs of same and opposite spin type.

An important ingredient in VMC is the optimization of the variational parameters of the wave function.¹⁰ For an efficient optimization of the variational parameters, we need the derivative of the energy with respect to these parameters. Our wave function is complex-valued, so we need to generalize the result for the real case²⁴ to read:

$$\begin{aligned} \frac{\partial E}{\partial \alpha_k} &= \frac{\partial}{\partial \alpha_k} \frac{\int \Psi^* \mathcal{H} \Psi d\Theta}{\int |\Psi|^2 d\Theta} \\ &= \frac{1}{\int |\Psi|^2 d\Theta} \int [\Psi^* \mathcal{H} \Psi + (\Psi^* \mathcal{H} \Psi)^*] d\Theta \\ &\quad - \frac{1}{(\int |\Psi|^2 d\Theta)^2} \int \Psi^* \mathcal{H} \Psi d\Theta \\ &\quad \quad \times \int [\Psi^* \Psi' + (\Psi^* \Psi')^*] d\Theta \\ &= \frac{2}{\int |\Psi|^2 d\Theta} \Re \int |\Psi|^2 \left(\frac{\Psi'}{\Psi} \right)^* \frac{\mathcal{H} \Psi}{\Psi} d\Theta \\ &\quad - \frac{2}{(\int |\Psi|^2 d\Theta)^2} \Re \int |\Psi|^2 \frac{\Psi'}{\Psi} d\Theta \int |\Psi|^2 \frac{\mathcal{H} \Psi}{\Psi} d\Theta \\ &= 2\Re \left\langle \left(\frac{\Psi'}{\Psi} \right)^* E_L \right\rangle - 2\Re \left\langle \frac{\Psi'}{\Psi} \right\rangle \langle E_L \rangle, \quad (21) \end{aligned}$$

where $\Psi' \equiv \partial \Psi / \partial \alpha_k$ and $d\Theta \equiv d\theta_1, \dots, d\theta_N$. In the second line of the equation we have used the fact that the Hamiltonian \mathcal{H} is Hermitian and real. The angle brackets denote an average over the probability distribution $|\Psi|^2$. This notation is also used in the following. In our wave function, the parameters α_i are inside an exponential, real-valued Jastrow factor:

$$\Psi = D_\uparrow D_\downarrow e^{J(\Theta, \alpha)}, \quad J \in \mathbb{R}, \quad (22)$$

where $\Theta \equiv (\theta_1, \dots, \theta_N)$, $\alpha \equiv (\alpha_1, \dots, \alpha_M)$. As a result we have:

$$\frac{\Psi'}{\Psi} = J', \quad J' \equiv \frac{\partial J}{\partial \alpha_k}. \quad (23)$$

Using Eq. (23) we can rewrite Eq. (21) as

$$\frac{\partial E}{\partial \alpha_k} = 2\Re \left[\left\langle J' E_L \right\rangle - \left\langle J' \right\rangle \langle E_L \rangle \right]. \quad (24)$$

Eq. (24) can only be used for cases where the Hamiltonian of the system is local. For this reason, it needs to be modified for the nonlocal contact interaction. One should note that even calculating the expectation value of the contact interaction is nontrivial. However, it can be calculated using translational invariance. We can divide the Hamiltonian into two parts:

$$\mathcal{H} = \mathcal{T} + \mathcal{V}_\delta, \quad \mathcal{V}_\delta = 2\pi V_\delta \sum_{i < j}^N \delta(\theta_{ij}), \quad (25)$$

where \mathcal{T} is the kinetic energy operator and \mathcal{V}_δ is the potential energy operator for the contact interaction. The kinetic energy is found in the same way as for the Coulomb case but we must modify the way we calculate the expectation value of the potential energy. We use $\Psi_{i \rightarrow j}$ to indicate that $\theta_i = \theta_j$. For a given wave function Ψ and a single potential term $\delta(\theta_{12})$ we have:

$$\begin{aligned} \langle \Psi | \delta(\theta_{12}) | \Psi \rangle &= \frac{\int |\Psi|^2 \delta(\theta_{12}) d\Theta}{\int |\Psi|^2 d\Theta} \\ &= \frac{\int d\theta_1}{\int d\theta_1} \times \frac{\int |\Psi_{1 \rightarrow 2}|^2 d\theta_2 \dots d\theta_N}{\int |\Psi|^2 d\Theta} \\ &= \frac{\int |\Psi_{1 \rightarrow 2}|^2 d\Theta}{2\pi R \int |\Psi|^2 d\Theta} \\ &= \frac{\int |\Psi|^2 \left| \frac{\Psi_{1 \rightarrow 2}}{\Psi} \right|^2 d\Theta}{2\pi R \int |\Psi|^2 d\Theta} \\ &= \frac{1}{2\pi R} \left\langle \left| \frac{\Psi_{1 \rightarrow 2}}{\Psi} \right|^2 \right\rangle. \quad (26) \end{aligned}$$

The same applies to a general term $\delta(\theta_{ij})$ if we replace 1 and 2 by i and j , respectively. One should note that similar formula can be used for the contact density in positron-electron systems, see Ref. 25.

The trial wave function for a nonlocal potential can be optimized in the same way as in the local case. The only difference is in the way we calculate the partial derivative $\partial E / \partial \alpha_k$. By combining the derivations of Eq. (21) and

Eq. (26) and using the property given by Eq. (23) we get:

$$\begin{aligned}
\frac{\partial E}{\partial \alpha_k} &= \frac{2}{\int |\Psi|^2 d\Theta} \Re \int \Psi^* \mathcal{H} \Psi' d\Theta \\
&- \frac{2}{(\int |\Psi|^2 d\Theta)^2} \Re \int \Psi^* \mathcal{H} \Psi d\Theta \int \Psi^* \Psi' d\Theta \\
&= \frac{2}{\int |\Psi|^2 d\Theta} \Re \int |\Psi|^2 J' \left(\frac{\mathcal{T}\Psi}{\Psi} + \mathcal{V}_\delta \right) d\Theta \\
&- \frac{2}{(\int |\Psi|^2 d\Theta)^2} \Re \int |\Psi|^2 \left(\frac{\mathcal{T}\Psi}{\Psi} + \mathcal{V}_\delta \right) d\Theta \int |\Psi|^2 J' d\Theta \\
&= \frac{2V_\delta}{R} \sum_{i < j}^N \left[\left\langle J'_{i \rightarrow j} \left| \frac{\Psi_{i \rightarrow j}}{\Psi} \right|^2 \right\rangle - \left\langle J' \right\rangle \left\langle \left| \frac{\Psi_{i \rightarrow j}}{\Psi} \right|^2 \right\rangle \right] \\
&+ 2\Re \left[\left\langle J' \frac{\mathcal{T}\Psi}{\Psi} \right\rangle - \left\langle J' \right\rangle \left\langle \frac{\mathcal{T}\Psi}{\Psi} \right\rangle \right], \quad (27)
\end{aligned}$$

where one should pay special attention to the asymmetry in the two terms in the double sum.

When the ground state wave function has been optimized, we can use it to find the pair distribution function and the angular momentum distribution of the electrons. The pair distribution function is very simple to find in VMC. We are interested in distances between electrons and all of these have values within $[0, \pi]$. This interval is divided into segments of equal size. The number of segments determines the spatial resolution. The distances between all the electron pairs in a configuration are calculated. These are then stored to the counters of the appropriate segments. We record separately the distances between pairs of spin-up electrons, pairs of spin-down electrons, and pairs of electrons with opposite spins. This procedure is repeated for consecutive configurations of the system to give a histogram of the distribution of electron distances. Finally the histogram is normalized appropriately.

The angular momentum distribution is found from the diagonal elements of the one-body density matrix in the basis of the natural orbitals. The natural orbitals diagonalize the density matrix, and for this system they are plane waves. Because of permutation symmetry, all the electrons in the system with the appropriate spin can be used simultaneously to calculate the diagonal matrix element. To allow a Monte Carlo evaluation we rewrite the integral as:

$$\rho_{ii,\sigma} = \left\langle \sum_{n=1}^{N_\sigma} \int \phi_i^*(\theta_n) \phi_i(\theta'_n) \frac{\Psi(\dots, \theta'_n, \dots)}{\Psi(\dots, \theta_n, \dots)} d\theta'_n \right\rangle, \quad (28)$$

where $\rho_{ii,\sigma}$ are the diagonal matrix elements, N_σ is the number of electrons of spin σ , and ϕ_i are the plane waves with angular momentum l_i . We normalize Eq. (28) as $\sum_i \rho_{ii,\sigma} = N_\sigma$. The average occupation of a single-particle state with angular momentum l_i and spin σ is given by $\rho_{ii,\sigma}$. The integral over $d\theta'_n$ can be evaluated as a sum over a grid with M points.

III. RESULTS

A. Coulomb interaction

Before presenting the actual results for the Coulomb interaction case, we first present an analysis of the accuracy of the ED method used. The only approximation done in our ED calculations is that we have a finite number of determinants in our expansion of the many-electron wave function. The actual number used is finally limited by the available computer resources. To give an idea of the accuracy of ED, we show in Fig. 1 the convergence of the $N = 6$, $S = 0$ ground state energy with increasing basis size M . The interaction strength is $V_C = 10$ making this the worst-case scenario for the convergence. We have increased M in steps of four, because the energy is lowered most when a new pair of $\pm l$ angular momentum values are included for both spin types. In this case, the maximum number of basis functions we have used is $M = 34$. For these values of M and N , $\binom{M}{N} = 1344904$. However, many configurations can be rejected from symmetry requirements, as we can force S_z and L to have certain fixed values. This use of symmetry leads to a final size of the Hamiltonian matrix of around 16000×16000 . We have fitted the energies using a function $E(M) = E_0 + \alpha \exp(-\beta M)$, giving the greatest weight to the most accurate points. In doing this, the $M = 18$ energy has only 2% of the weight of the $M = 34$ one. We can estimate the truly exact, full basis energy from this fit to be $E_0 \approx 122.60$. This is rather close to the energy of 122.638 found for $M = 34$, especially if it is compared to the Hartree-Fock energy of 152.32 or the VMC one of $122.866 \pm .004$. This comparison shows that the ED accuracy is clearly sufficient to test the quality of our VMC approach.

A crucial part of the VMC wave function is the selection of the single-particle states in the Slater determinants. For a weak interaction, the occupations in the noninteracting many-body states can be used. In this limit, the electrons arrange so as to minimize the total kinetic energy. This means that the single-particle states are occupied as compactly as possible around the $l = 0$ state. The resulting configurations are shown in the upper part of Fig. 2. Each box in this figure represents one single-particle state, having angular momentum from $l = 0$ at the bottom, up through $l = \pm 1, \pm 2, \dots$, with increasing energy. For four electrons, the second shell formed by the angular momentum $l = \pm 1$ states is half-filled, and the exchange energy favors spin-polarization of the two electrons in that shell. One should note that the configurations shown are also the most important ones in the ED expansion of the wave function. When the interaction strength grows, the relative importance of the kinetic energy decreases with respect to the interaction energy and the rule for the occupations changes. The strongly interacting electrons favor closed shells for each spin type, i.e., either a half-filled shell of one spin type or a closed shell, and possibly a finite spin polariza-

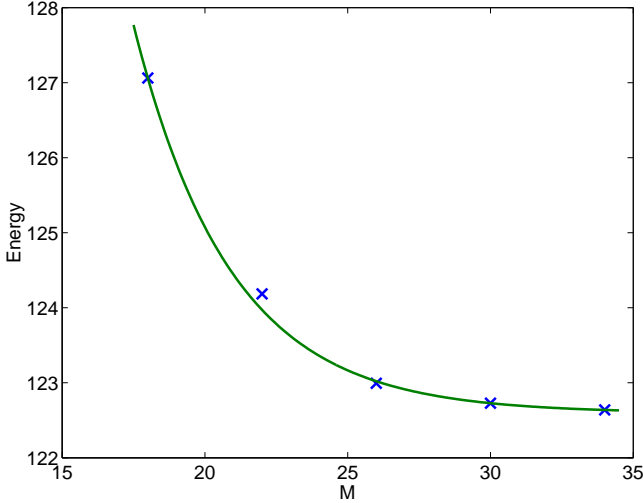


FIG. 1: Convergence of the ground state energy as a function of basis size M , for the case of $N = 6$ electrons and a strong interaction, $V_C = 10$. The line shows a fit of the form $E_0 + \alpha \exp(-\beta M)$, in which the most accurate energies have the largest weight.

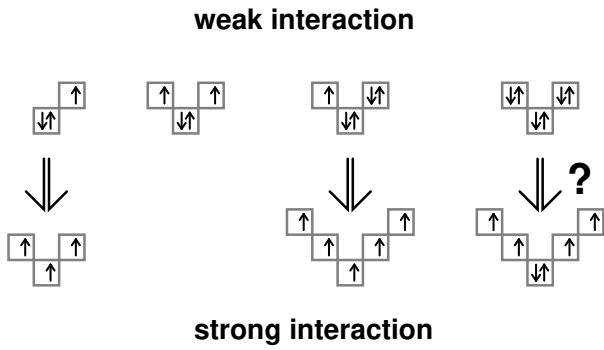


FIG. 2: Single-particle states occupied in the VMC wave function. These are also the most important configurations in the ED expansion.

tion. An example of this is the $N = 3$ case, where the only minority-spin electron flips its spin and moves to a higher angular momentum state, see Fig. 2. A similar type of transition, but involving two electrons, occurs in the $N = 5$ case. Again, the resulting configuration has closed shells of one spin type. The situation for $N = 6$ electrons is not fully clear. The VMC results show that the system is in a half-filled configuration with maximum S_z for a strong interaction. However, one must be careful in making such a statement since the wave function, and thus the energy, of the spin-polarized configuration is more accurate than that of the $S = 0$ configuration. The ED energy difference between this state and the closed-shell state (both shown in Fig. 2) is too small to allow any conclusions to be drawn.

TABLE I: Percentages of correlation energy captured by VMC. The error in the last digit is given in parentheses.

V_C	$N = 2$	$N = 3$	$N = 4$	$N = 5$	$N = 6$
0.1	0.987(2)	0.888(6)	0.966(9)	0.900(4)	0.937(7)
1	0.9960(4)	0.992(2)	0.9838(5)	0.9505(5)	0.9652(6)
10	0.99991(1)	0.9982(2)	0.9975(1)	0.9900(1)	0.9922(1)

Next, we will show a detailed comparison of the ED and VMC predictions for various observables of the system containing a number of electrons ranging from $N = 2$ to $N = 6$. We consider three different interaction strengths, $V_C = 0.1, 1$, and 10 . We begin with the results for the ground state energy. Here a convenient measure of the quality of the trial wave function is the percentage of correlation energy captured by VMC, defined as

$$E_C = \frac{E_{\text{HF}} - E_{\text{VMC}}}{E_{\text{HF}} - E_{\text{ED}}} , \quad (29)$$

where E_{HF} is the Hartree-Fock energy. The results are shown in Table I and indicate that VMC becomes more accurate when the interaction becomes stronger. These results might be surprising, but one reason is that the Hartree-Fock method is rather accurate for weak interaction, and fails seriously in the limit of strong interaction. A second observation is that the VMC approach seems to become less accurate as the number of particles grows. This is due to the fact that Hartree-Fock is more accurate for larger particle numbers. For example, in the $V_C = 0.1$ case, the change in correlation energy when the number of particles is increased from two to six particles is two orders of magnitude less than the change in total energy.

The cases where VMC performs worst are those when the determinants correspond to an open-shell. For the worst case, $N = 3$ and $V_C = 0.1$, we have been able to calculate the overlap of the VMC wave function with the exact one, and the result is 0.998, which is surprisingly accurate. The Hartree-Fock overlap is 0.985. The “failure” of VMC in the open shell case can be understood as follows: Without the Jastrow factor, the VMC wave function is simply the most important ED configuration. The multiplication with a Jastrow factor generates a wave function that can also be expanded in the ED determinantal basis. In Fig. 3 we show three configurations which have the largest weights in the many-electron wave function of the system. The second and third configurations are obtained from the most important configuration by exciting a pair of spin up and down electrons to higher angular momentum states, thus changing their relative angular momentum. In VMC, configurations that have opposite change in relative angular momentum compared to the major configuration, $\Delta(l_\uparrow - l_\downarrow) = \pm n$, have the same weight in the expansion. In ED they do not in the case of an open shell. This is the crucial difference between the ED and VMC wave functions, shown in Fig. 3. It turns out that if the most important con-

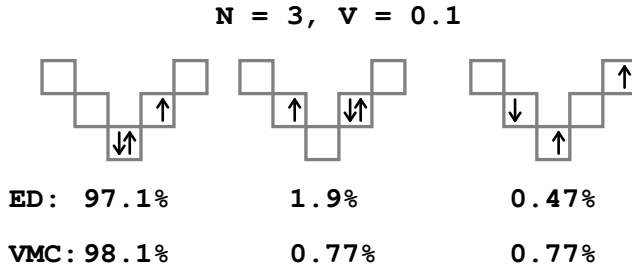


FIG. 3: The most important configurations and their weights in the ED and VMC wave functions for $N = 3$ weakly interacting electrons, $V_C = 0.1$.

figuration has a closed shell, then it is symmetric with respect to a change of sign of all the angular momentum values $l \rightarrow -l$. In addition, all other configurations should have the same property, meaning that a configuration pair that is related by a rule $l \rightarrow -l$ have the same weight. This symmetry is correctly built into the VMC wave function in a closed-shell case, but incorrectly in the case of an open shell.

To have a more detailed comparison, we show in Fig. 4 the occupations of the single-particle states. It shows clearly that the occupations agree very well in all cases. In addition, VMC becomes more accurate when the interaction grows stronger, as in the case of energies above. The form of the occupations still resembles the noninteracting step function when the interaction strength is low ($V_C = 1$). For strong interaction ($V_C = 10$), however, the occupations are rather smeared. We also see that the distribution of the only minority spin is spread over several single-particle states. This is especially true for the $N = 6$, $V_C = 10$ case, where the probability of finding the electron in the $l = 0$ state is only around a fourth of the HF value. One could expect the VMC occupations to become less accurate for strong interactions, because the construction of the VMC wave function starts from a single configuration, which is later multiplied by a Jastrow factor. This is not the case, and it is very difficult to see any deviation in the VMC occupation numbers that would show such a single-configuration limitation. From this, one can conclude that the Jastrow factor is very efficient in capturing the essential correlation effects induced by the interaction between electrons. One might also question the importance of the determinant part of the VMC wave function. We believe that having a good choice for this is crucial for the success of the VMC simulation. Even if the weight of this single configuration is not large in the exact expansion when the interaction is strong, it specifies the symmetry of the VMC many-body state. One should note that this is also the case for quantum dots, where the noninteracting single-particle states can also be used in the determinant part of the VMC wave function, and they are even the optimal ones in the case of a closed-shell configuration.¹⁰ The reason, both in quantum rings and dots, is the high symmetry of the problem: In a parabolic dot, the center-of-mass and

relative motion decouple, also in the many-body wave function. Thus if one starts from a noninteracting state that is a ground state of the center-of-mass motion, the interactions only change the relative motion part of the many-body wave function. This means that if a Slater-Jastrow wave function is used, the Slater determinant part is not changed by the interaction between electrons. The case of a quantum ring is similar in the sense that the center-of-mass and relative motion also decouple, but now because of the translational invariance of the system.

Finally, the pair-correlations are shown in Fig. 5. Also here the agreement is rather good. However, in the case of $N = 6$ and $V_C = 1$, one can see a deviation of the VMC and ED data around $\pi/2 \leq \theta \leq \pi$. This large θ regime is not very important energetically, as the Coulomb interaction is much weaker there than at small θ . This is, however, important for the long-range nature of the system. In the case in question, the system behaves in an anti-ferromagnetic fashion in both theories. VMC is much more accurate in the case of four electrons where the system has finite spin polarization and no anti-ferromagnetic ordering. When the interaction is made stronger, the VMC and ED data agree very nicely. Both theories indicate that the system has a wigner-molecule-like structure, with electrons localized equidistantly on a ring. One should note that in this case, also the long-range physics is accurately described by the VMC wave function.

B. Contact interaction

The accuracy of the ED method for the contact interaction case is not as good as for the Coulomb case. This can be seen in Fig. 6, where we show the total energy as a function of the basis size M for a two-electron ring using both contact and Coulomb interaction between electrons. We have used interaction strength $V_C = 1$. As the energies are on very different scales, we have scaled them by setting the values at $M = 6$ ($M = 62$) to be one (zero), correspondingly. The inset of Fig. 6 shows the total energy of the contact interaction case as a function of the inverse of M . One can see that the energy is linear for small $1/M$.

For larger particle numbers, we are not able to reach such a large basis set as mentioned above. For this reason, the results are less reliable than those of the Coulomb case. The main objective of this Section is then to demonstrate that the energy gradient of Eq. (27) is correct and can be used for optimization. In doing this, the $N = 4$ with $V_\delta = 1$ is a suitable test case, as the ED energy is still reasonably accurate. Of course, the energy for the $N = 2$ case would be even more accurate, but this case is too simple to be convincing.

Fig. 7 shows the derivative of the total energy with respect to the parameter a , plotted as a function of a . We have used Eq. (27) for calculating this. One can see that the derivative is zero at $a \approx 2.2$. This value agrees well with the total energy minimum, as one can see in

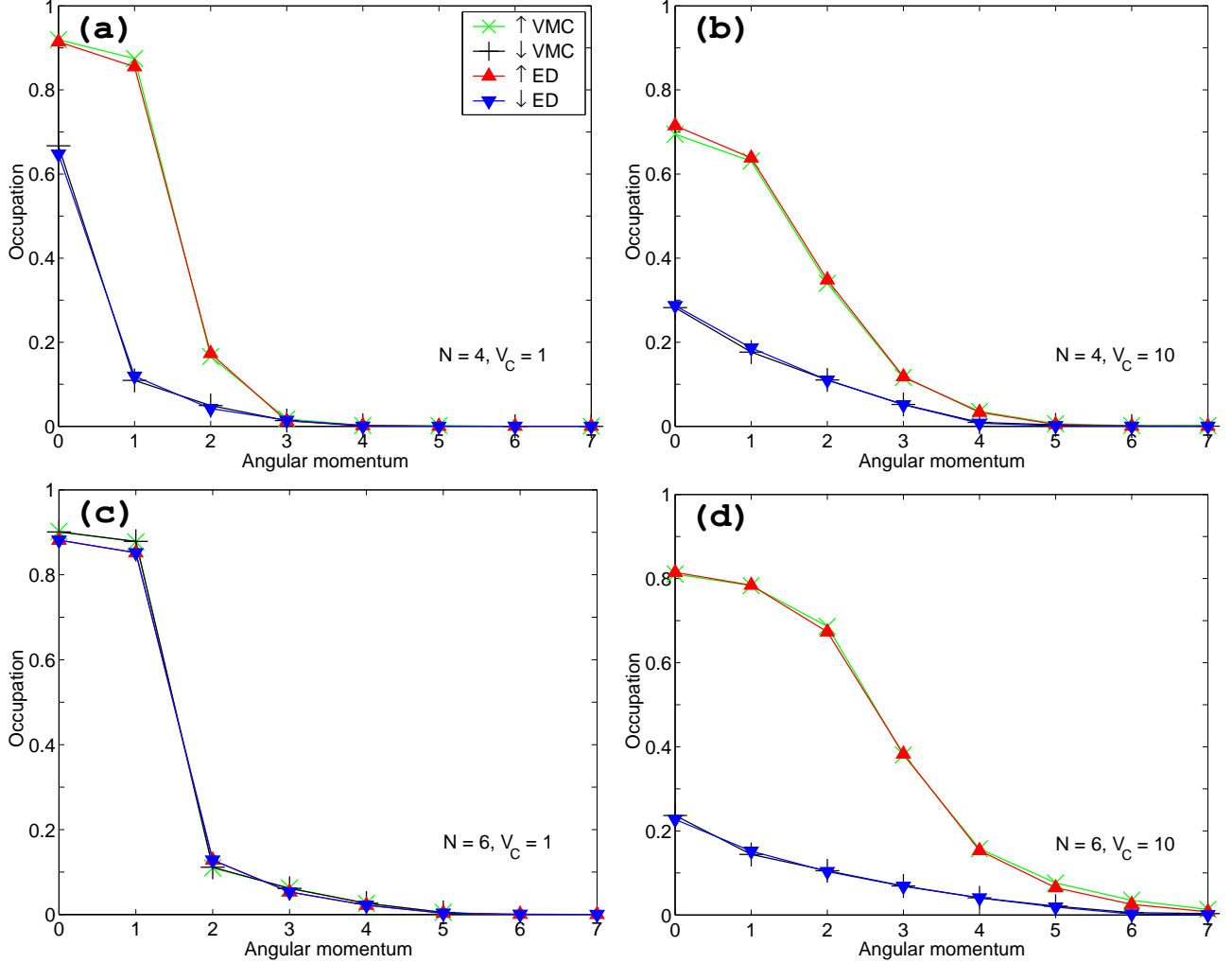


FIG. 4: Occupation of the single-particle states from ED and VMC for both up- and down-spin electrons. The upper panel shows results for $N = 4$ electrons for interaction strength (a) $V_C = 1$ and (b) $V_C = 10$. The lower panel shows results for $N = 6$ for (c) $V_C = 1$ and (d) $V_C = 10$. The occupations are rather close to the Fermi distribution for the $V_C = 1$ cases, but at $V_C = 10$ the distribution is already rather smooth at the Fermi step of the noninteracting system. The agreement between ED and VMC data is very good in all the cases considered here.

the insert of Fig. 7. One can conclude from this that the equation for the nonlocal energy derivative, derived above, gives a correct value. If one uses Eq. (21) that does not take into account the nonlocality of the Hamiltonian, one obtains the data shown by the dashed line in Fig. 7. It is clear that this energy derivative is seriously wrong and has a positive sign for the whole range shown.

We have used the gradient formula in the optimization of the wave function, and have reached the minimum shown above. We have used 10 fully independent Monte Carlo samplers (walkers) in the optimization, and calculated the expectation values of Eq. (27) over this set. The parameters are moved to the direction of the negative gradient, with damping on the step size that ensures convergence. More details on the efficient optimization of the VMC wave function can be found from Ref. 10. The optimal wave function captures 95.5(1)% of the correla-

tion energy. This is a lower number than for the $V_C = 1$ Coulomb case. Of course, one can not directly compare these numbers, but we also expect the Coulomb case to be more accurate than the contact interaction one. The reason for this is that the Jastrow factor $j(\theta)$ used here is a smooth function for a small inter-electron angle. This is correct for a regularized Coulomb-type interaction, as this interaction is constant for small inter-electron angles. On the other hand, the contact interaction only affects electrons that are on top of each other and for this reason it would be more realistic to include a cusp in the Jastrow factor used in the contact interaction case. This is not done here as we are more interested in the optimization of the wave function rather than obtaining accurate energies.

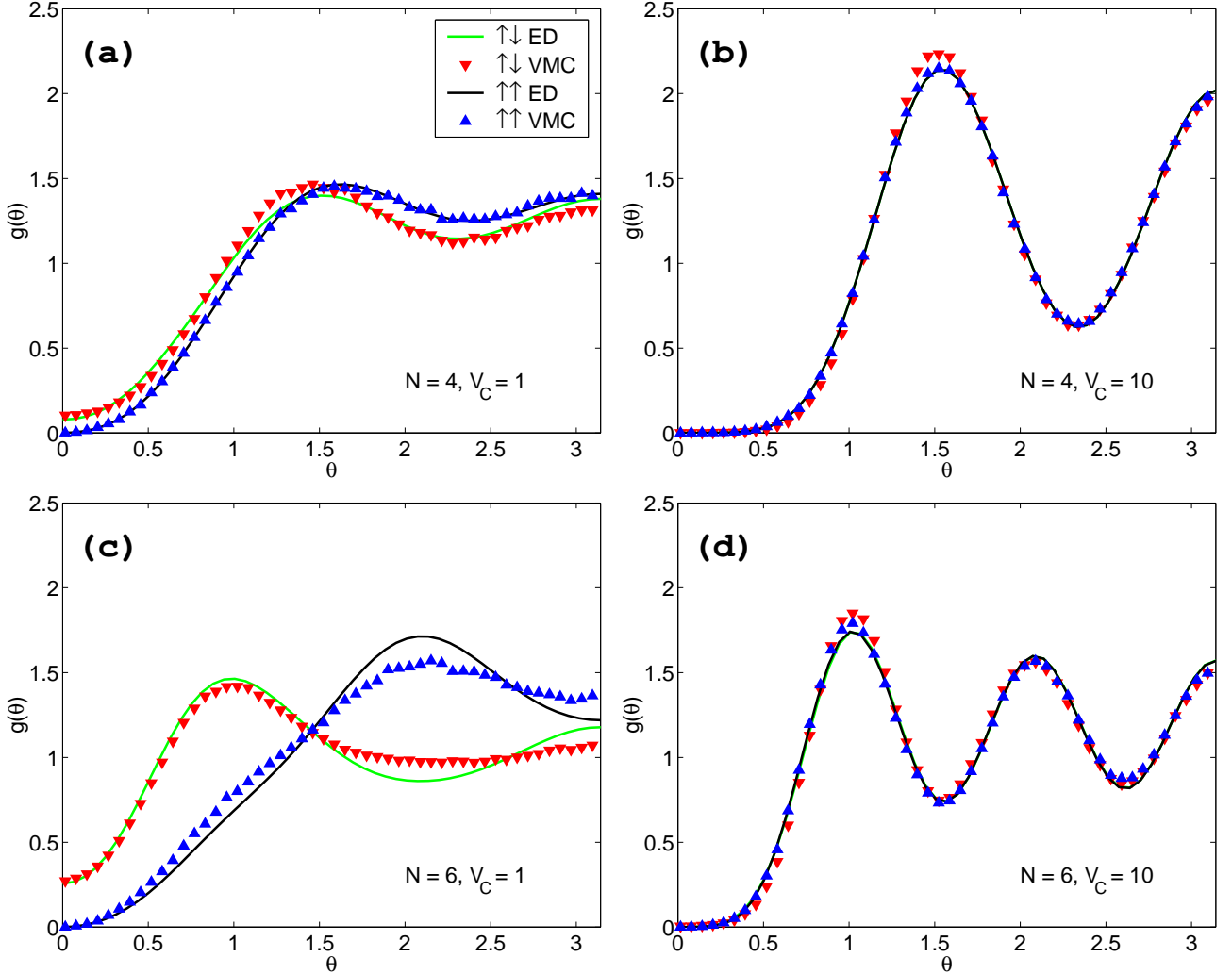


FIG. 5: Pair distribution function from ED and VMC for four and six electrons. The upper panel shows the results for $N = 4$ electrons for interaction strength (a) $V_C = 1$ and (b) $V_C = 10$. The lower panel shows results for $N = 6$ electrons for (c) $V_C = 1$ and (d) $V_C = 10$. The agreement is very good for all cases except (c), where the two methods give a different behavior for the range $\pi/2 < \theta < \pi$. This case shows an anti-ferromagnetic order in the system. The pair distribution function for the $V_C = 10$ cases has a structure that shows electron localization on the ring.

C. Mapping between Coulomb and contact interaction

As both Coulomb and contact interactions cause electrons to avoid each other, it is not unreasonable to believe that in some sense the eigenstate corresponding to the Coulomb interaction would be a good approximation for the eigenstate of the contact interaction. To utilize this notion we need a mapping between the interaction strengths V_δ and V_C , corresponding to the contact and Coulomb interaction, respectively. A simple possibility for this mapping is to use the angular momentum distribution since it characterizes the state of the system. The idea is that we would like to find the interaction strengths V_C and V_δ which give a similar state of the system. This can be done, e.g., by summing up the occupation prob-

abilities of states that are unoccupied in the noninteracting case. This measures the probability of particles being outside the noninteracting Fermi sphere. To make the comparison even simpler, we will do it below only for the majority spin type.

Fig. 8 shows the non-Fermi probability for the two interaction types in the four-electron case. This probability is zero when the interaction is off, and increases as a function of the strength of interaction. The two curves are rather similar up to interaction strength of around one, but after that the probability in the case of contact interaction saturates. This leads to a simple relation between the interaction strengths:

$$V_C(V_\delta) = \begin{cases} V_\delta & , V_\delta \leq 1 \\ 1 & , V_\delta > 1 \end{cases} \quad (30)$$

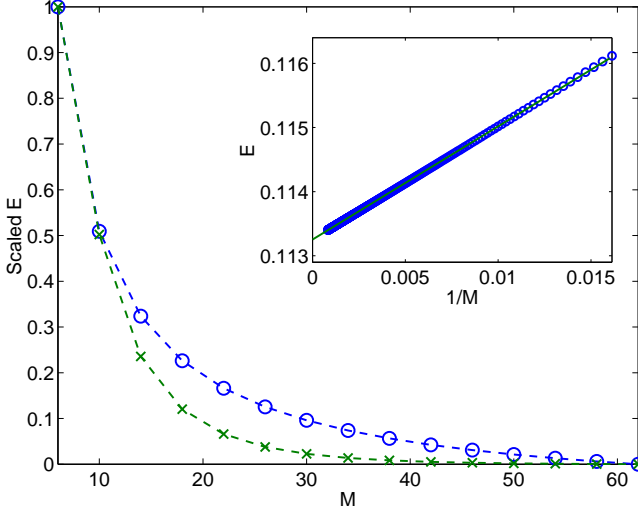


FIG. 6: Total energy (scaled, see text), for interaction of contact (circles) and Coulomb (crosses) type. The inset shows the total energy for the case of contact interaction for larger basis sizes.

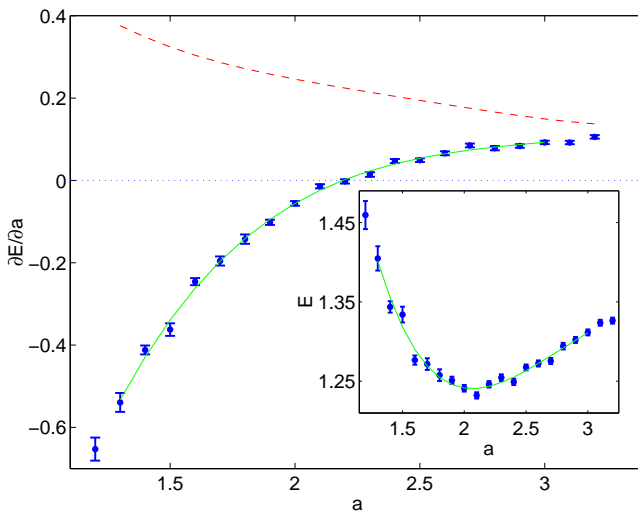


FIG. 7: Derivative of the total energy E with respect to the wave function parameter a , as a function of a (with error bars). The solid line is shown to guide the eye. The dashed line gives the wrong energy derivative which results from using Eq. (21) for a nonlocal Hamiltonian. The inset shows the total energy as a function of a . The energy is minimum around the parameter values where the gradient is zero.

A good way to measure the usefulness of this approach is to compare the actual energies of the contact interaction with the expectation values $\langle \psi_C | \mathcal{H}_\delta | \psi_C \rangle$. Here \mathcal{H}_δ is the Hamiltonian corresponding to the contact interaction with strength V_δ and $|\psi_C\rangle$ is the eigenvector of the Hamiltonian corresponding to the Coulomb interaction with interaction strength $V_C(V_\delta)$. This data, for both ED and VMC, is shown in Table II. Another obvious way to compare the two states is to calculate the overlap,

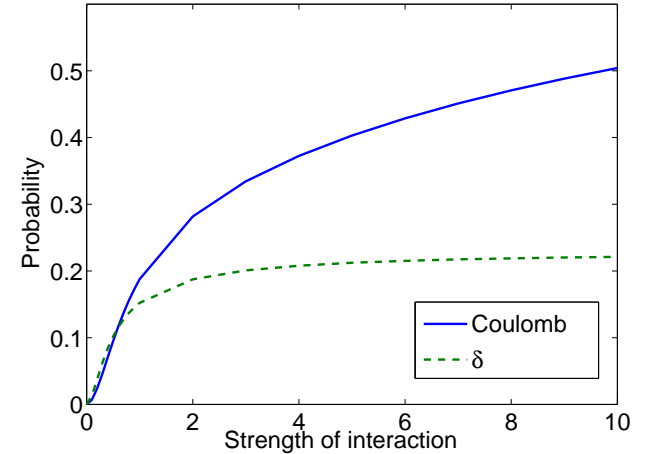


FIG. 8: The sum of the probabilities of the majority-spin electrons having orbital angular momentum outside the non-interacting Fermi sphere, as a function of the strength of interaction for a $N = 4$ electron quantum ring.

TABLE II: Results of a mapping between the contact and Coulomb interaction for both ED and VMC.

V_δ	ED			VMC
	E_δ	$\langle \psi_C \mathcal{H}_\delta \psi_C \rangle$	$\langle \psi_C \phi_\delta \rangle$	$\langle \psi_C \mathcal{H}_\delta \psi_C \rangle$
0.1	0.7337	0.7512	0.9984	0.750(1)
1	1.1627	1.3004	0.9795	1.378(7)
10	1.2711	2.6933	0.9820	2.625(5)

i.e., the inner product $\langle \phi_\delta | \phi_\delta \rangle$, also shown in Table II. One can see that the energy obtained with the Coulomb ground state is not very accurate for a strong interaction, even if the overlap has a reasonably high value. For weaker interactions, the agreement is much better. In all cases, the agreement between the ED and VMC data is satisfactory.

IV. SUMMARY AND CONCLUSIONS

We have studied interacting electrons in a quantum ring, using both a Coulomb-type and a contact interaction between the electrons. The ring was taken to be purely one-dimensional. We compared the results obtained from variational Monte Carlo with those of exact diagonalization. In VMC, the variational wave function was taken to be of a simple Slater-Jastrow form, a single determinant, the ground state of the noninteracting system, multiplied by a two-body correlation factor. The results obtained indicate that this simple wave function is able to capture the important correlation effects, and in most cases even with a high accuracy.

We also derived a formula for the energy derivative with respect to optimization parameters in the VMC wave function, in the case where the Hamiltonian is a nonlocal operator and showed that this formula can be

used to find the optimal values of the parameters.

In conclusion, a simple variational wave function combined with Monte Carlo techniques to calculate the optimal wave function and observables of the system results in an efficient computational strategy for interacting electrons in purely one-dimensional quantum rings. Since a similar conclusion can be drawn for two-dimensional quantum dots,¹⁰ we expect this to hold also for quantum rings of a finite width.

Acknowledgments

This work has been supported by the Academy of Finland through its Centers of Excellence Program (2000-2005). SSG acknowledges financial support from the Vilho, Yrjö, and Kalle Väisälä Foundation of the Finnish Academy of Science and Letters.

¹ U. F. Keyser, C. Fühner, S. Borck, R. J. Haug, M. Bichler, G. Abstreiter, and W. Wegscheider, Phys. Rev. Lett. **90**, 196601 (2003).

² A. E. Hansen, A. Kristensen, S. Pedersen, C. B. S. rensen, and P. E. Lindelof, Physica E **86**, 3120 (2001).

³ F. V. Kusmartser, J. Phys.: Condens. Matter **3**, 3199 (1991).

⁴ E. A. Jagla and C. A. Balseiro, Phys. Rev. Lett. **70**, 639 (1993).

⁵ F. V. Kusmartser, J. F. Weisz, R. Kishore, and M. Takahashi, Phys. Rev. B **49**, 16234 (1994).

⁶ K. Niemelä, P. Pietiläinen, P. Hyvönen, and T. Chakraborty, Europhys. Lett. **36**, 533 (1996).

⁷ P. S. Deo, P. Koskinen, M. Koskinen, and M. Manninen, Europhys. Lett. **63**, 846 (2003).

⁸ A. Emperador, F. Pederiva, and E. Lipparini, Phys. Rev. B **68**, 115312 (2003).

⁹ K. Hallberg, A. A. Aligia, A. P. Kampf, and B. Normand, Phys. Rev. Lett. **93**, 067203 (2004).

¹⁰ A. Harju, J. Low. Temp. Phys. **140**, 181 (2005).

¹¹ P. Borrmann and J. Harting, Phys. Rev. Lett. **86**, 3120 (2001).

¹² A. Harju, B. Barbiellini, S. Siljamäki, R. M. Nieminen, and G. Ortiz, Phys. Rev. Lett. **79**, 1173 (1997).

¹³ C. J. Umrigar and C. Filippi, Phys. Rev. Lett. **94**, 150201 (2005).

¹⁴ S. Sorella, Phys. Rev. B **71**, 241103 (2005).

¹⁵ U. F. Keyser, Ph.D. thesis, University of Hannover (2002).

¹⁶ E. Hylleraas, Z. Physik **48**, 469 (1928).

¹⁷ J. C. Slater, Phys. Rev. **34**, 1293 (1929).

¹⁸ E. U. Condon, Phys. Rev. **36**, 1121 (1930).

¹⁹ J. C. Slater, Phys. Rev. **38**, 1109 (1931).

²⁰ P.-O. Löwdin, Phys. Rev. **97**, 1474 (1955).

²¹ J. Oitmaa (2005), private discussion.

²² W. M. C. Foulkes, L. Mitas, R. J. Needs, and G. Rajagopal, Rev. Mod. Phys. **73**, 33 (2001).

²³ R. B. Laughlin, in *The Quantum Hall Effect*, edited by R. E. Prange and S. M. Girvin (Springer-Verlag, New York, 1987), pp. 233–301.

²⁴ X. Lin, H. Zhang, and A. M. Rappe, J. Chem. Phys. **112**, 2650 (2000).

²⁵ S. Chiesa, M. Mella, and G. Morosi, Phys. Rev. A **69**, 022701 (2004).